Immunity, Vol. 10, 51–61, January, 1999, Copyright ©1999 by Cell Press

Crystal Structure of an MHC Class I Presented Glycopeptide that Generates Carbohydrate-Specific CTL

Jeffrey A. Speir,* Ussama M. Abdel-Motal,‡ Mikael Jondal,‡§ and Ian A. Wilson*†§
*Department of Molecular Biology
†The Skaggs Institute for Chemical Biology
The Scripps Research Institute
10550 North Torrey Pines Road
La Jolla, California 92037
‡Microbiology and Tumorbiology Center
Karolinska Institutet
P.O. Box 280
S-171 77 Stockholm
Sweden

Summary

T cell receptor (TCR) recognition of nonpeptidic and modified peptide antigens has been recently uncovered but is still poorly understood. Immunization with an H-2K^b-restricted glycopeptide RGY8-6H-Gal$_2$ generates a population of cytotoxic T cells that express both α/β TCR, specific for glycopeptide, and γ/δ TCR, specific for the disaccharide, even on glycolipids. The crystal structure of K^b/RGY8-6H-Gal$_2$ now demonstrates that the peptide and H-2K^b structures are unaffected by the peptide glycosylation, but the central region of the putative TCR binding site is dominated by the extensive exposure of the tethered carbohydrate. These features of the K^b/RGY8-6H-Gal$_2$ structure are consistent with the individual ligand binding preferences identified for the α/β and γ/δ TCRs and thus explain the generation of a carbohydrate-specific T cell response.

Introduction

The dogma of exclusive T cell recognition of peptide-major histocompatibility complex (pMHC) antigens has recently been challenged (Kaufmann, 1996; Melian et al., 1996; Porcelli et al., 1996; Carbone and Gleeson, 1997; Kihlberg and Elofsson, 1997). Cells presenting nonpeptidic or modified peptide antigens (e.g., glycopeptides and glycolipids bound to class I and II MHC, and MHC class I–like CD1 molecules, respectively) can also be recognized by cytotoxic T cells (CTL) bearing α/β or γ/δ T cell receptors (TCR) (Beckman et al., 1994; Davis and Chien, 1995; Sieling et al., 1995; Chien et al., 1996; Kaufmann, 1996; reviewed by Porcelli et al., 1998). However, the structural properties of these unconventional TCR ligands are currently undetermined except for the crystal structure of mouse CD1 (Zeng et al., 1997).

Conventional T cell recognition of pMHC has been widely studied (Eisen et al., 1996; Davis et al., 1998) and now includes the recent high-resolution crystal structures of intact α/β TCR-pMHC complexes (Garboczi et al., 1996; Garcia et al., 1996, 1998; Ding et al., 1998). The TCR binds the pMHC surface in a diagonal orientation in which a majority of the intermolecular interactions are derived from contact of CDRs 1 and 2 of both TCR polypeptide chains with highly conserved MHC α_1 and α_2 helical residues. The TCR α and β chain hypervariable CDR3 loops are ideally positioned within the MHC helices to examine the contents of the peptide binding groove and hence are well suited for their role in peptide-antigen recognition. The consistent diagonal orientation of the TCRs over the pMHC so far observed allows more accurate prediction of the structural determinants of MHC-bound ligands that are likely to be responsible for T cell recognition (reviewed by Wilson and Garcia, 1997).

The biological role of antigen ligation by γ/δ TCR in T cell–mediated immunity is far less understood. Indeed, MHC-independent recognition of ligands by γ/δ TCRs was anticipated after analysis of their primary structures. Similar to the comparison between immunoglobin (Ig) V_H and V_L CDR3 loops, the TCR δ chain CDR3s are significantly longer and more heterogenous in length than those of the γ chain (Rock et al., 1994). The TCR α and β chain CDR3s are both long and homogeneous in length. Therefore, the γ and δ chain pairings suggest γ/δ TCR antigen binding is more closely related to that of Ig molecules than to α/β TCR (Rock et al., 1994; Davis and Chien, 1995). Many γ/δ T cell effector functions overlap with those of α/β T cells; however, γ/δ T cells differ in their antigens and mode of ligand recognition that may be reflected in their localization, relative population, and activation kinetics (Kaufmann, 1996; Boismenu and Havran, 1997).

Glycosylation is a common posttranslational modification of proteins to be secreted or transported to the cell surface (Varki, 1993). Nevertheless, evidence for the processing of glycoproteins to glycopeptides and subsequent glycopeptide presentation by MHC class I (MHC I) or II (MHC II) receptors during normal immune responses is scarce (Carbone and Gleeson, 1997; Kihlberg and Elofsson, 1997). Glycosylated fragments of collagen type II presented by MHC II I-A^q (Broddefalk et al., 1998) and the O-linked glycosylation of cytosolic and nuclear proteins with a single N-acetylglucosamine (GlcNAc) (Hart et al., 1989; Haurum et al., 1994) represent two possible sources of natural glycopeptides for T cell recognition.

Studies using synthetic glycopeptides have enhanced our understanding of oligosaccharide recognition by T cells (Carbone and Gleeson, 1997; Kihlberg and Elofsson, 1997). The ability of T cells to recognize carbohydrates has important implications, as some glycoprotein and glycolipid-associated oligosaccharides have been identified as tumor-associated antigens (TAA; Hakomori, 1989). In the first demonstration of a T cell response to a naturally occuring glycan, immunization with synthetic MHC I restricted peptides conjugated with GlcNAc generated glycopeptide-specific CTL (Haurum et al., 1994). Although many studies have demonstrated the fine specificity of helper T cells and CTL for glycopeptide versus carrier peptide, they have not convincingly demonstrated TCR recognition of the carbohydrate

§To whom correspondence should be addressed (email: mikael.jondal@mtc.ki.se [M. J.], wilson@scripps.edu [I. A. W.]).

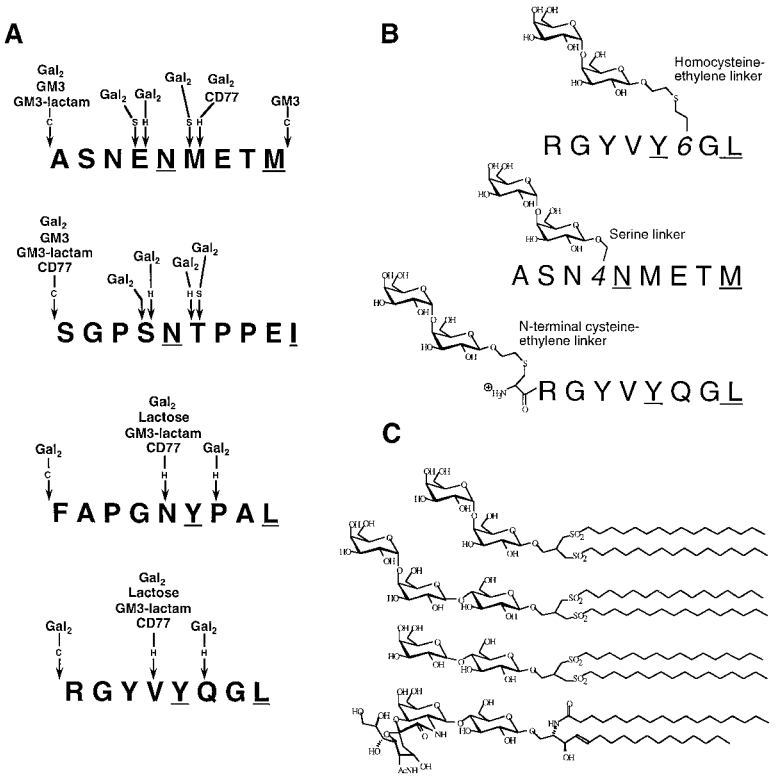

Figure 1. Glycosylated MHC I Peptide Epitopes and Glycolipids Tested for Carbohydrate-Specific T Cell Generation and Recognition

(A) Sequence of glycosylated viral peptides of H-2D^b (top two) or H-2K^b (bottom two). The amino acids replaced by chemical linkers (H, homocysteine-ethylene; S, serine; C, cysteine-ethylene) are denoted by the arrows connected to the attached carbohydrates. The term "homocysteine" will refer to the homocysteine-ethylene linker throughout. The primary anchor residues of each peptide are underlined. Glycopeptide names are given as the first three amino acids of the carrier peptide and its residue length, followed by the linker position and type, then the coupled carbohydrate abbreviation. Thus, ASN9-4H-Gal$_2$ is the D^b nonapeptide with galabiose (Gal-α(1,4)Gal-β) coupled to position 4 via a homocysteine linker.

(B) Structures of the three types of chemical linkers, which are conjugated with galabiose in this illustration. The glycopeptides shown are, from top to bottom, RGY8-6H-Gal$_2$, ASN9-4H-Gal$_2$, and CRG9-1C-Gal$_2$.

(C) Chemical structures of selected glycolipids synthesized with the same carbohydrate moieties present in the glycopeptides; they are, from top to bottom, Gal$_2$-bisulfone, CD77-bisulfone, Lactose-bisulfone, and GM3-lactam ceramide.

hapten moiety independent of the restricting MHC background or carrier peptide. We have found that immunization with MHC I H-2K^b restricted glycopeptide RGY8-6H-Gal$_2$ (Figure 1) can generate polyclonal CTL that specifically kill cells presenting the glycopeptide-MHC complex (gpMHC) as well as a glycolipid with the galabiose oligosaccharide as the hydrophilic head group (Abdel-Motal et al., 1996). Fractionation of the CTL population by TCR expression has shown glycopeptide-specific killing is mediated by α/β T cells (60% of the CTL), and glycolipid-specific killing by γ/δ T cells (10%–15% of the CTL). The MHC-restricted α/β T cell response to the glycopeptide, and gpMHC-unrestricted, hapten-specific response of γ/δ T cells correlate well with the antigen recognition abilities of each T cell subset.

Although their biological properties have been elucidated, the structures of MHC-presented glycopeptides have not. Structural analysis is essential since a majority of the synthetic glycopeptides that have been tested have failed to generate carbohydrate-specific T cell responses (Kihlberg and Elofsson, 1997). Glycopeptides with centrally located oligosaccharides, such as RGY8-6H-Gal$_2$, have clearly been the most immunogenic (Abdel-Motal et al., 1996). Therefore, we determined the crystal structure of the H-2K^b/RGY8-6H-Gal$_2$ complex at 2.2 Å resolution to identify the structural determinants critical for T cell activation. The RGY8-6H-Gal$_2$ glycopeptide structure shows that glycan position, linker length, and carbohydrate size are important for recognition and discrimination by the different T cells and can be rationalized with the recently determined footprint of the α/β T cell receptor over the pMHC (Garboczi et al., 1996; Garcia et al., 1996, 1998; Ding et al., 1998).

Results

Chemical Characteristics of the Glycopeptides and Glycolipids

The known MHC allele-specific motifs (Rammensee et al., 1995) and available crystal structures of K^b (Fremont et al., 1992) and D^b (Young et al., 1994) were utilized in glycopeptide synthesis and design (Figure 1). The D^b-binding peptides were ASNENMETM from PR8 influenza virus nucleoprotein (NP) (van Bleek and Nathenson, 1990) and SGPSNTPPEI from adenovirus Ad5EI protein (Rammensee et al., 1993). The K^b-binding peptides were FAPGNYPAL from Sendai virus NP (Schumacher et al., 1991) and RGYVYQGL from vesicular stomatitis virus (VSV) NP (van Bleek and Nathenson, 1990). The allele-specific anchor residues for K^b and D^b are centrally located at P5 for D^b and P5 (8-mer) or P6 (9-mer) for K^b (Figure 1).

Five carbohydrates differing in size and chemical structure were coupled either to serine, cysteine, or homocysteine (Figure 1). Oligosaccharide CD77 is the Burkitt lymphoma TAA (Nudelman et al., 1983). Lactose and GM3-lactam are also tumor-associated saccharides (Holmes et al., 1987; Nores et al., 1987). Galabiose (Gal-α(1,4)-Galβ or Gal$_2$) is an integral part of several natural glycolipid head groups and is the terminal disaccharide of CD77 (Figure 1). The amino acid glycans replaced upward-pointed residues flanking the central anchor in the K^b or D^b peptides or were added to their termini (Figure 1; Abdel-Motal et al., 1995, 1996).

Peptide binding to MHC I was unaffected by the glycan modifications (Abdel-Motal et al., 1996), and the stability of the glycopeptides in vivo has been previously

Table 1. Cell Surface Carbohydrate (CHO) Exposure and Specificity of CTL Raised against Glycopeptide Immunogens

MHC Class I	Immunogen	Peptide, Glycopeptide, or Glycolipid Antigen[a]	CHO Detection[b]	Cytotoxicity[c]		
				Whole	α/β^-	γ/δ^-
K^b	RGY8-4H-Gal_2	RGY8-4H-Gal_2	++	+++		
		RGY8-4H		+		
	RGY8-6H-Gal_2	RGY8-6H-Gal_2	+++	+++	−/+	+++
		RGY8-6H		+		
		Gal_2-bis sulfonlipid	+++	++	++	−/+
		CD77-bis sulfonlipid	+++	+		
		GM3-lactam ceramide	+++	−		
		Lactose-bis sulfonlipid		−		
	RGY8-4H-CD77	RGY8-4H-CD77	+	++		
		RGY8-4H		+		
	RGY8-4H-GM3-lactam	RGY8-4H-GM3-lactam	+++	++		
		RGY8-4H		+		
D^b	ASN9-4H-Gal_2	ASN9-4H-Gal_2	++	−/+		
		ASN9-4H		−/+		
	ASN9-6H-Gal_2	ASN9-6H-Gal_2	+++	+		
		ASN9-6H		+		
	ASN9-6H-CD77	ASN9-6H-CD77	−	−		
		ASN9-6H		−		

The data are summarized from Abdel-Motal et al. (1996). Blank slots indicate the data are undetermined.

[a] See Figure 1 legend for an explanation of the glycopeptide and glycolipid nomenclature. Antigens without a carbohydrate abbreviation represent the carrier peptide stripped of carbohydrate.

[b] Mean fluorescence intensity (MFI) from flow cytoflourometric analysis of glycopeptide-treated RMA-S cells or glycolipid-coated EL-4 cells. Measurement of corresponding anti-carbohydrate MAb binding with FITC-labeled rabbit anti-mouse Ig is given on a relative logarithmic scale from − to +++. The different levels are 50–100 (+), 100–250 (++), and 300–400 (+++) above control background. The IgM MAb specific for CD77 did not bind well to the trisaccharide conjugated to either peptide.

[c] Generated CTL were tested against peptide, glycopeptide, or glycolipid-coated EL-4 target cells as described (Abdel-Motal et al., 1996). Killing (^{51}Cr-release) above background is given on a scale from − to +++. The different levels are 1%–5% (−/+), 5%–25% (+), 25%–50% (++), and more than 50% (+++) specific target cell lysis above background. The RGY8-6h-Gal_2 and Gal_2-bisulfonlipid antigens were also examined with CTL populations depleted of either α/β (α/β^-) or γ/δ (γ/δ^-) T cells using magnetic Dynabeads coated with specific anti-framework MAb.

demonstrated (Abdel-Motal et al., 1993). Monoclonal antibody (MAb) detection of the peptide-linked carbohydrates on the cell surface differed depending on the position of the glycan substitution on the peptide and linker length. Thus, antibody binding to the peptide glycans provided a measure of the carbohydrate exposure in the various pMHC complexes. Carbohydrates attached at internal positions in the peptide by the serine linker were poorly detected by anti-carbohydrate MAb. In contrast, high carbohydrate exposure was detected for all of the glycopeptides that had N-terminal cysteine-ethylene extensions or with the homocysteine linker at internal positions with one exception (ASN9-6H-CD77, Table 1). The anti-CD77 MAb is of the IgM type and may not be optimal for binding to CD77 in the context of the pMHC. Carbohydrate headgroups in all of the glycolipids, after liposomal transfer to EL-4 target cells, were highly exposed at the cell surface and stable for at least 24 hr under tissue culture conditions, as detected with the corresponding anti-carbohydrate MAb (Abdel-Motal et al., 1996).

Specificity of α/β and γ/δ CTL toward Glycopeptides and Glycolipids

Immunizations with the glycopeptide panel produced a wide range of T cell responses (Table 1; Abdel-Motal et al., 1996). Glycosylation of the peptide termini, glycopeptides with internal serine-coupled oligosaccharides, and D^b-binding glycopeptides produced low CTL responses in general with no evidence for any carbohydrate specificity. In contrast, K^b-binding glycopeptides, RGY8-4H-Gal_2 and RGY8-6H-Gal_2, with central homocysteine-coupled galabiose generated strong bulk CTL responses that specifically killed glycopeptide-coated target cells (Table 1; Figure 1). Fractionation of the RGY8-6H-Gal_2 generated T cell population based on α/β or γ/δ TCR expression determined glycopeptide-specific killing was primarily by the α/β T cells (Table 1). Interestingly, the bulk CTL generated with RGY8-6H-Gal_2 also killed target cells coated with D^b-binding glycopeptides containing homocysteine-coupled galabiose (e.g., ASN9-6H-Gal_2), and suggested a strict carbohydrate specificity independent of the pMHC background (Abdel-Motal et al., 1996).

MHC-unrestricted carbohydrate specificity was unambiguously determined by fusing liposomes composed of galabiose containing glycolipid (Figure 1C) with EL-4, YAC-I, and P815 cells. These glycolipid-coated target cells were specifically killed by a small γ/δ T cell subpopulation present in the bulk CTL generated against RGY8-6H-Gal_2 (Table 1). These data suggest that the α/β and γ/δ T cells recognized different portions of the same gpMHC antigen that correlates with their specific killing of glycopeptide-coated or glycolipid-coated target cells, respectively. Thus, we determined the H-2K^b/RGY8-6H-Gal_2 crystal structure to improve our understanding of carbohydrate recognition by T cells.

RGY8-6H-Gal_2 Glycopeptide Structure

The crystal structure of K^b/RGY8-6H-Gal_2 was determined using well-developed procedures for K^b pMHC

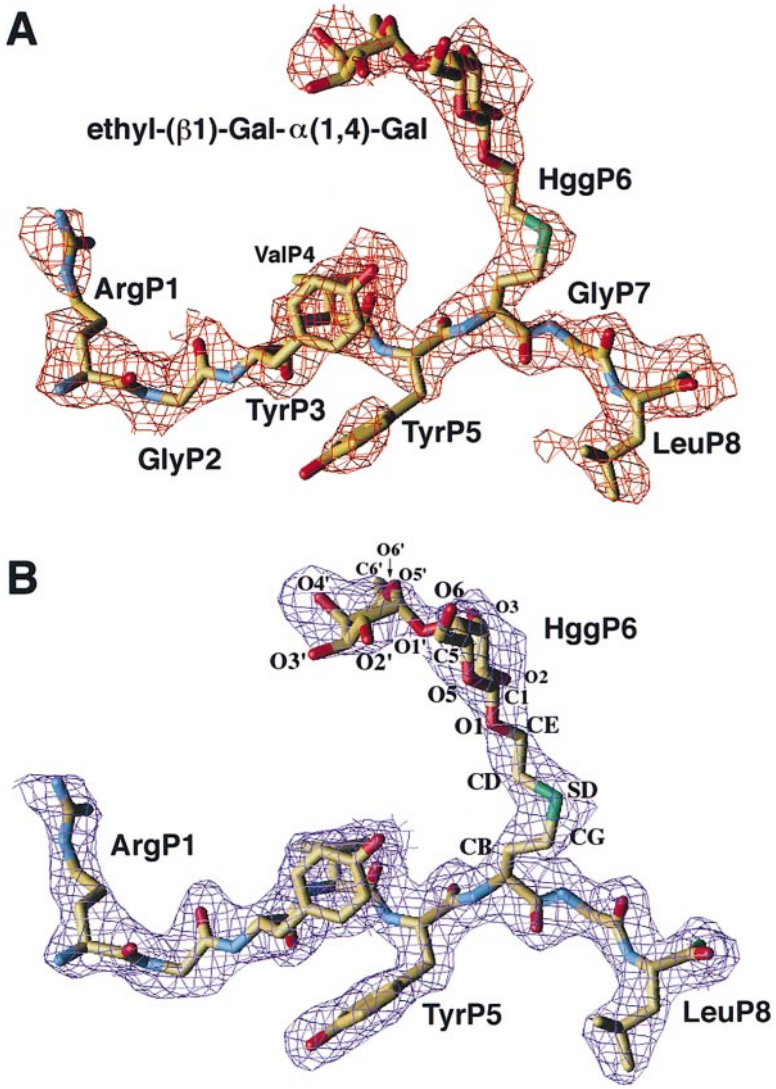

Figure 2. Glycopeptide Electron Density in the H-2K^b Binding Groove

(A) Shaken (McRee, 1993), σ_A-weighted (Read, 1986) F_o-F_c map contoured at 1.5σ. The map was computed before refinement of the glycopeptide model; the final coordinates colored by atom type (C, yellow; O, red; N, cyan; S, green) are shown in the electron density.

(B) Final shaken and σ_A-weighted $2F_o$-F_c map contoured at 1σ. A 2.5 Å cover radius has been applied to the density in both maps. Atom O6′ is out of view behind the terminal galactose in this view.

complexes (see Experimental Procedures). The final model included the H-2K^b/glycopeptide complex, four well-ordered N-linked carbohydrates to the MHC, and 108 waters (R_{cryst} 22.4%, R_{free} 27.9%). Electron density for RGY8-6H-Gal$_2$ was continuous and well resolved, allowing unambiguous modeling of the glycosylated peptide (Figure 2). The glycopeptide structure is nearly identical to that of K^b-bound VSV-8 for the common residues (P1-P5, P7-P8) (Fremont et al., 1992). The root-mean-square deviation (r.m.s.d) is only 0.19 Å for the equivalent polyalanine atoms between VSV-8 and RGY8-6H-Gal$_2$ after the Cα atoms of the K^b $\alpha_1\alpha_2$ superdomains are aligned. Many interactions between the glycopeptide and MHC heavy chain, including water-mediated hydrogen bonds, are also shared with the K^b/VSV-8 complex (Table 2); however, the glycosidic modification makes RGY8-6H-Gal$_2$ the largest MHC I bound antigen to have its structure determined to date. The homocysteine galabiose glycan at position 6 of the peptide (HggP6) extends 12 Å above the peptide backbone (Figures 3A and 3B). Arginine, the longest unmodified amino acid, can only extend approximately 7 Å out from the peptide backbone (e.g., see ArgP1 in Figures 2 and 3). Interestingly, there are no significant alterations of the K^b structure as a result of glycopeptide binding.

The conformation of the galabiose thioether linker loosely matches that of VSV-8 GlnP6 for the first few equivalent atom positions and orients HggP6 toward the α_2 helix (Figure 3B). HggP6 "leans" on the α_2 helix, creating several contacts unique to the glycopeptide (Table 2), but does not make any hydrogen bonds. In the absence of T cell receptor ligation or any direct hydrogen bonds to the linker or sugars from the K^b $\alpha_1\alpha_2$ domains, the polar and hydrophobic contacts are the only interactions stabilizing the placement of the glycosidic modification adjacent to the α_2 helix.

The contacts between the disaccharide and K^b are mainly with the internal galactose residue. Only a single contact exists between the K^b α_2 domain and the terminal galactose (Table 2); in fact, both sugars of the galabiose are clasped between the MHC α_2 helix and the β_2m subunit of a neighboring K^b molecule in the crystal lattice. The neighboring β_2m is on the opposite side of galabiose from the α_2 helix. Two hydrogen bonds and

Table 2. Glycopeptide Interactions with H-2K[b]

Glycopeptide		MHC	Code[b]	Glycopeptide		MHC[a]	Code[b]
ArgP1	N	Tyr7 OH	P		SD	Glu152 OE2	V
		Tyr171 OH	P			Glyβ43 O*	P
	O	Tyr159 OH	H		CD	Glu152 OE2	V
	NH1	Arg62 NE	P		CE	Glyβ43 C, CA, O*	V
GlyP2	N	Tyr7 OH	P		O1	Glu152 OE2	P
		Glu63 OE1	H			Arg155 CD	V
	O	Lys66 NZ	H			Arg155 NE	P
TyrP3	O	Asn70 ND2	H		O2	Leuβ40 CD2*	V
		Wat99-Glu24 OE2	H			Glyβ43 O*	P
	OH	Glu152 OE1	H			Argβ81 NH1*	P
		Arg155 NE, NH2	P		O3	Argβ81 NH1*	H
ValP4	O	Arg155 NH1	H		C5	Ala150 O	V
		Arg155 NH2	H		O5	Arg155 CD	V
TyrP5	N	Asn70 OD1	H		O2'	Arg155 CG	V
	O	Wat43-Asn70 OD1	H		C6'	Lysβ83 NZ*	V
		Wat43-Ser73 OG	H		O6'	Argβ81 NE*	P
		Wat43-Wat80	H			Argβ81 NH1*	P
	OH	Ser99 OG	P			Argβ81 NH2*	P
HggP6[c]	N	Arg155 NH2	P			Lysβ83 CE*	V
	O	Trp147 CZ2	V			Lysβ83 NZ*	H
		Wat5-Asp77 OD1	H	**GlyP7**	O	Trp147 NE1	H
	CB	Glu152 CD	V	**LeuP8**	N	Asp77 OD2	H
		Glu152 OE1	V		O	Tyr84 OH	H
		Glu152 OE2	V			Thr143 OG1	H
		Arg155 NH2	V		OT	Wat87-Asp77 OD2	H
	CG	Trp147 CD1	V			Wat87-Thr80 OG1	H
		Trp147 NE1	V				

[a] Residues marked with an asterisk are from the β_2-microglobulin domain (β) of a neighboring molecule in the crystal.
[b] H, hydrogen bond; P, polar interaction; V, van der Waals interaction (only listed for HggP6). Polar interactions are defined as van der Waals interactions between highly electronegative atoms. The distance and geometry criteria for hydrogen bonds are the defaults used in HBPLUS (McDonald and Thornton, 1994). When a hydrogen bond is made from the glycopeptide to the MHC via a bridging water, all hydrogen bonds from the water to the MHC are listed (e.g., Wat43). The maximum distance allowed for polar or van der Waals interactions is 4.3 Å.
[c] Hgg is the abbreviation for homocysteine galabiose glycan. Hgg, with selected atoms labeled, is shown in Figure 2.

several polar interactions between HggP6 and neighboring β_2m residues Leuβ40, Glyβ43, Argβ81, and Lysβ83 are a result of the galabiose entrapment (Table 2). These interactions may be preventing the formation of other hydrogen bonds between galabiose and K^b.

The peptide-conjugated galabiose retains a structure very similar to that of the free disaccharide (Svensson et al., 1986). Superposition of the small molecule galabiose crystal structure with the HggP6-linked disaccharide structure gives an r.m.s.d of only 0.78 Å. The two galabiose structures differ mainly due to a 46° difference between their internal glycosidic dihedral angles, presumably due to contact of the HggP6 galabiose with the neighboring β_2m molecule; the terminal galactose in HggP6 must rotate away from the neighboring β_2m molecule to avoid forming energetically unfavorable close contacts.

Disaccharide Exposure and Mobility

The galabiose disaccharide is 71% exposed to solvent in the crystal structure. The orientation adopted by HggP6 places most of its mass into the open space between the $\alpha_1\alpha_2$ helices. Thus, the overall exposed surface area of the glycopeptide is substantially greater than that of normal peptides bound by K^b and other MHC I antigens (see Figures 3D and 3E). Contact between glycopeptide residue HggP6 and the α_2 helix also contributes to significantly more K^b-buried surface in the glycopeptide complex (952 $Å^2$) than in K^b/VSV-8 (843 $Å^2$).

Modeling studies of this complex show that the galabiose exposure could be even greater. Torsion angles for the relatively long thioether-hydrocarbon linker are largely unrestricted. Small rotations ($<20°$) of just two of the linker torsion angles can free the galabiose from any contact with the K^b α_2 helix (Figure 3C). The repositioned galabiose would be 100% solvent accessible giving the glycopeptide nearly double the exposed peptide surface area of other MHC-bound peptides (383 $Å^2$ versus 150–220 $Å^2$). Galabiose-specific monoclonal antibodies strongly recognize RGY8-6H-Gal_2 treated RMA-S cells (Abdel-Motal et al., 1996), providing further evidence for the high exposure of the glycopeptide-attached galabiose. The MAb could possibly recognize the galabiose in close proximity to the MHC helices, but small haptens are more commonly buried deep within the immunoglobin combining site (reviewed by Wilson and Stanfield, 1994). The unrestricted access to the galabiose is compatible with antibody binding of small haptens and therefore supports the likelihood of HggP6 conformations that fully expose the carbohydrates (e.g., Figure 3C).

Carbohydrate Dominance of the TCR Footprint

An extended glycan linker, such as that observed in the RGY8-6H-Gal_2 crystal structure, will place the galabiose well above the peptide backbone in the pMHC region normally covered by the α/β TCR CDR3 loops (Garboczi

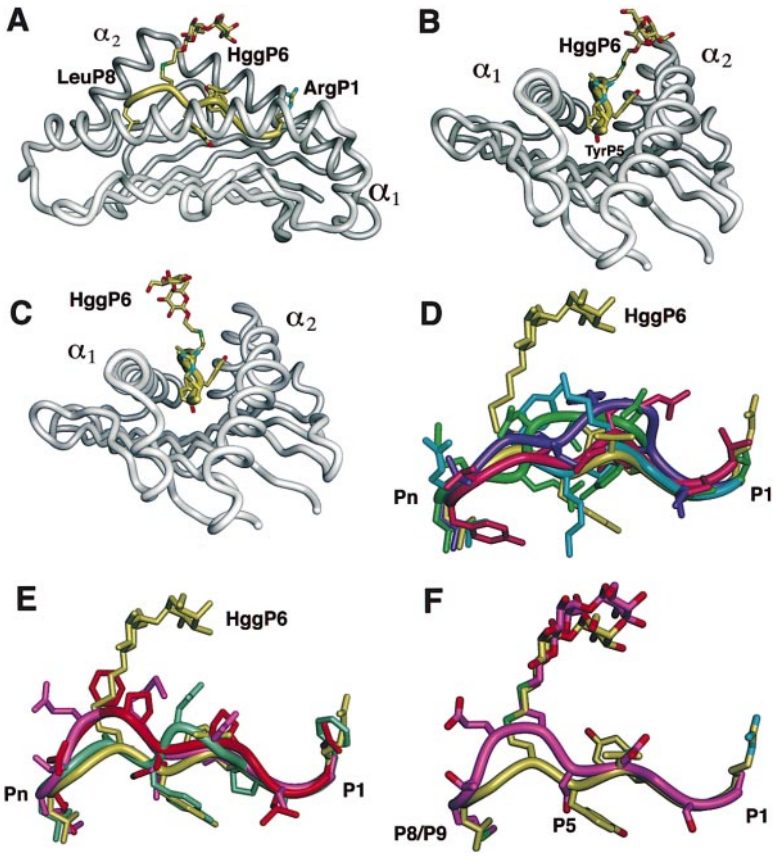

Figure 3. The H-2K^b Glycopeptide Complex Structure and Comparison with Other MHC I–Bound Peptides and Modeled Glycopeptides

(A) The K^b/RGY8-6H-Gal$_2$ crystal structure showing the glycopeptide colored by atom type (see Figure 2) and MHC $\alpha_1\alpha_2$ superdomain (residues 1–180) in light gray viewed from the side and (B) along the peptide binding groove. (C) A model derived from the crystal structure in which only very small rotations about the HggP6 linker torsion angles dramatically change the level of TCR access to the carbohydrate (compare to B). (D) The greater size and exposure of the carbohydrate component of RGY8-6H-Gal$_2$ shown in comparison with other MHC I peptide ligands (the PDB accession codes and references are given in Experimental Procedures). The superpostions are the result of aligning only the C$^\alpha$ atoms of the MHC $\alpha_1\alpha_2$ domains and then comparing the positions of the bound peptides. RGY8-6H-Gal$_2$ is yellow. The other human MHC I bound peptides are: purple, HLA-A2/Influenza M1; cyan, HLA-B8/HIV1 GAG 7r; green, HLA-B53/HIV2 GAG; and pink, HLA-B35/HIV1 NEF. (E) A similar comparison of RGY8-6H-Gal$_2$ (yellow) with other murine MHC I bound peptides: red, L^d/QL9; magenta, D^b/Infl NP; and light green, K^b/SEV-9. (F) A model of D^b-bound ASN9-6H-Gal$_2$ superimposed with RGY8-6H-Gal$_2$.

et al., 1996; Garcia et al., 1996, 1998; Ding et al., 1998). Torsion angle rotations of the linker can result in large lateral movements of the galabiose; however, the central peptide attachment site, combined with the diagonal orientation of the TCR over the MHC binding groove, still keeps the galabiose within the CDR3 region of the TCR footprint. Therefore, direct interactions between the RGY8-6H-Gal$_2$ carbohydrates and the TCR CDR3 loops are relatively convincing.

The current position of the disaccharide in the K^b/RGY8-6H-Gal$_2$ crystal structure would place it under the CDR3β loop and next to a key β chain contact patch on the MHC α_2 helix (residues 149–158). TCR recognition of the galabiose, therefore, would predominantly involve the β subunit. The area between the glycopeptide and the α_1 helix is more accessible and could allow TCR α and β subunit contacts directly to the peptide backbone as well as to the side chains. TCR corecognition of glycopeptide and MHC residues in this manner favors an MHC-restricted, glycopeptide-specific α/β T cell response, and may explain the low-level bulk CTL cross-reactivity to the carrier peptide stripped of carbohydrate.

The highly exposed galabiose also closely matches the attributes of preferred γ/δ T cell antigens that supports the dichotomy of the anti-RGY8-6H-Gal$_2$ T cell response. Direct, immunoglobin-like recognition of the galabiose, either as a highly exposed glycopeptide hapten or glycolipid headgroup, is easily conceivable. Complete carbohydrate exposure can be achieved by varying the HggP6 conformation (e.g., Figure 3C) or may be induced through TCR binding. A great variety of TCR docking scenarios and HggP6 conformations appear feasible, and could potentially coexist in vivo, which would explain the simultaneous generation of carbohydrate-specific γ/δ CTL and glycopeptide-specific α/β CTL by RGY8-6H-Gal$_2$.

Discussion

Important Structural Features of the K^b/Glycopeptide Complex

The crystal structure of H-2K^b-bound RGY8-6H-Gal$_2$ reveals the VSV-8 carrier peptide and K^b structures are unaffected by the peptide glycosylation; thus, the novel features of the glycopeptide presentation are specifically localized to the carbohydrate portion of the ligand. Indeed, the glycan modification places the galabiose disaccharide at the outer limits of the MHC peptide binding groove where it abuts the apex of the α_2 helix, well beyond the reach of normal peptide side chains. The galabiose is secured at this position more by intermolecular crystal contacts to a neighboring β_2m molecule than by intramolecular contacts to the MHC receptor, suggesting that HggP6 may have significantly more conformational freedom in solution.

The chemical structure, P6 substitution site, and size of the Hgg linker favor a highly exposed hapten moiety in virtually any linker conformation. This unusual access to an MHC I bound ligand allows for direct TCR interactions with the galabiose, which is considerably larger than an amino acid side chain. Alterations in the shape

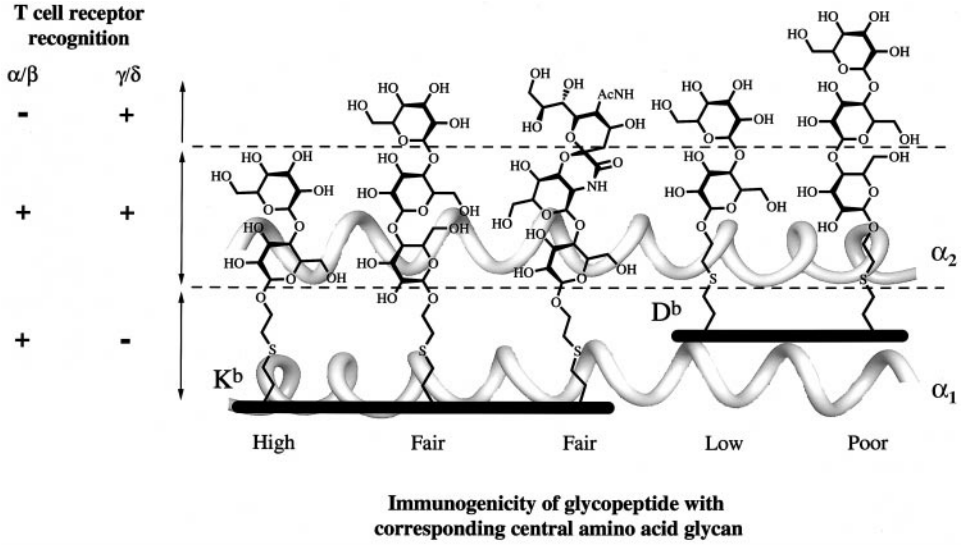

Figure 4. The Proposed Relationship between Peptide Glycan Structure and Specfic TCR Recognition

In this model, the α/β TCR simultaneously binds the MHC, peptide, and glycan, whereas the γ/δ TCR binds only the glycan. The highest positions reached by the MHC α_1 and α_2 helices are represented by the helical ribbons in the background. The glycans are assumed to be substituted for single, central, and outward pointing peptide residues and to have nearly fully extended conformations. The glycans shown represent (from left to right) H-galabiose, H-CD77, and H-GM3-lactam on a K^b bound 8-mer, and H-galabiose and H-CD77 on a D^b-bound 9-mer (see Figure 1). The extent of exposure (vertical axis) is correlated with generation of reactive CTL (horizontal axis) as outlined in Table 1 and Abdel-Motal et al. (1996). Note that high glycan exposure does not necessarily guarantee good immunogenicity since α/β TCR corecognition of the pMHC is disfavored and the glycan is less likely to have a defined antigenic structure outside of the MHC binding groove suitable for γ/δ TCR recognition.

of the TCR combining site, such as large conformational adjustments of the CDR3 loops, may be required for a TCR to bind the K^b/RGY8-6H-Gal_2 disaccharide compared to a pMHC. Movements of up to several angstroms by CDRs 1α, 3α, and 3β were observed in comparisons between the free and bound structures of the murine 2C TCR (Garcia et al., 1998). It is likely that CDR flexibility is also involved, although to a lesser extent, in the high-affinity allorecognition of the H-2L^d/QL9 peptide complex by the 2C TCR. A model of the 2C/L^d interaction (Speir et al., 1998) reveals that a bulge near the QL9 C terminus, as a result of a ridge in the L^d binding groove floor, is likely to greatly increase the TCR contact with the QL9 peptide and require different conformations of the 2C CDRs for optimal binding compared to the syngeneic 2C/dEV8/K^b complex. Alternatively, HggP6 may adopt a conformation that places the carbohydrate into a cavity between the TCR α and β chains (Garcia et al., 1996) or generally between the TCR and pMHC, requiring little to no structural adjustments of either receptor. Indeed, the TCR-pMHC interfaces are extensive but exhibit poor shape complementarity, leaving large cavities between the contacting surfaces (Garboczi et al., 1996; Ding et al., 1998; Garcia et al., 1998). Regardless of the poorly formed TCR-pMHC interface, central modifications of the peptide antigen that extend outward from the MHC binding groove will create new and more numerous contacts with the TCR.

Glycopeptide Structure-Function Relationships: A Beginning

MHC I and II bound peptide immunogens with glycosylation sites outside of the central peptide residues normally fail to generate glycopeptide-specific CTL (Abdel-Motal et al., 1996; Kihlberg and Elofsson, 1997). It is now apparent that glycans at these positions would not promote contact between carbohydate haptens and the hypervariable CDR3 loops of an α/β TCR, leading to the killing of both carrier peptide and glycopeptide coated target cells by the CTL generated against glycopeptides with noncentral glycan modifications (Ishioka et al., 1992; Abdel-Motal et al., 1996; Kihlberg and Elofsson, 1997).

Glycosylation of the central peptide residues places the carbohydrates within the expected TCR CDR3α and 3β footprint and yields glycopeptides whose immunogenicity is dependent upon the linker length and carbohydrate size. Glycopeptides incorporating disaccharides or larger carbohydrates linked to serine showed weak CTL immunogenicity, as well as poor detection by carbohydrate-specific MAb on the cell surface (Abdel-Motal et al., 1996). In contrast, GlcNAc monosaccharides coupled to peptides with serine linkers generate CTL that are able to discriminate between the glycosylated and native peptides, as well as between chemically similar glycopeptides (Haurum et al., 1994). The fine specificity demonstrated in T cell recognition of the GlcNAc-based glycopeptides suggests monosaccharides attached to short linkers near the peptide center are better suited for glycopeptide-specific α/β TCR recognition. From the K^b/RGY8-6H-Gal_2 structure, it appears the greater mass of the serine-linked disaccharides and larger carbohydrates will be confined to the limited space between the MHC helices and thus may interfere with TCR-MHC interactions and/or hinder specific-recognition of the carbohydrates by the TCR. The smaller size of monosaccharides is less likely to disrupt α/β TCR interactions within the MHC binding site, but their relatively low exposure disfavors a carbohydrate-specific γ/δ T cell response (Figure 4).

Longer oligosaccharide tethers, such as homocysteine, can fully expose bound carbohydrates (Figures 3 and 4). The greater exposure results in facilitated MAb detection of the sugars and strong generation of carbohydrate-specific CTL (Abdel-Motal et al., 1996), presumably through direct interaction between TCRs and the carbohydrates. Furthermore, the unobstructed access to the glycan is probably a key factor in generating an MHC-unrestricted γ/δ T cell response. Several cross-reactive T cell clones to MHC bound peptides with chemically TNP-modified lysine residues have been described (Martin et al., 1992). TNP exposure, when attached to lysine, would be equivalent to that of homocysteine-linked galabiose, and could be responsible for the immunodominance of the TNP epitopes and restriction of the responding T cell repertoire (Hochgeschwender et al., 1987). Furthermore, the specificity of the cross-reactive T cells only for TNP-lysine located near the center of the peptide, and the freedom of one TNP-specific T cell hybridoma from class II polymophism, mirrors the behavior of carbohydrate-specific CTL (Martin et al., 1992; Kohler et al., 1997). Thus, central placement and extensive exposure are common factors in MHC antigens that produce enhanced cross-reactivity, reduced MHC restriction, and hapten-specfic recognition by the responding T cell population.

Poor or Diminished CTL Reactivity to Large Oligosaccharides and D^b-Bound Galabiose

D^b-bound glycopeptides with homocysteine linked galabiose (e.g., Figure 3F) are poorly immunogenic, and K^b-bound glycopeptides presenting homocysteine-linked CD77 or GM3-lactam are less immunogenic than RGY8-6H-Gal_2 (Table 1; Abdel-Motal et al., 1996). Interestingly, these glycopeptide designs could place carbohydrate structures further above the MHC $\alpha_1\alpha_2$ helices than observed in K^b/RGY8-6H-Gal_2 (Figure 4), as CD77 and GM3-lactam are larger than galabiose by one sugar unit or more. In addition, the D^b-binding glycopeptides have a large arch in the peptide backbone near the C terminus that would futher elevate glycans attached to the bulged residues (Figures 3F and 4; Young et al., 1994).

Peptide antigen recognition by α/β TCR normally occurs within the $\alpha_1\alpha_2$ helices and may, therefore, fail to entirely encompass these large glycans. Furthermore, carbohydrates outside or atop the $\alpha_1\alpha_2$ helices are likely to disrupt conserved TCR-MHC interactions that are important to the docking, orientation, and proper register of the TCR on the pMHC molecule and hence can explain the reduced, poor, or lack of CTL reactivity to these glycopeptides (Table 1).

γ/δ T Cell Response to Glycolipid

The K^b/RGY8-6H-Gal_2 crystal structure supports the possibility of distinct γ/δ CTL stimulation through MHC-unrestricted γ/δ TCR recognition of the exposed carbohydrate haptens. Indeed, the γ/δ T cells may be directly triggered by corresponding galabiose-presenting glycolipids fused with target cells (Abdel-Motal et al., 1996). However, it is unknown whether MHC-unrestricted antigen binding by γ/δ TCR allows triggering and clonal expansion of γ/δ CTL in the present system.

Less exposed oligosaccharides may also be capable of generating γ/δ CTL, but peptide and MHC residues are more likely to be in close proximity to these carbohydrates and may inhibit γ/δ TCR binding. Interestingly, the inherent linker flexibility of HggP6 in RGY8-6H-Gal_2 may provide the glycan with the ability to switch between the positions and/or structures best recognized by the two types of TCR, providing a rationale for the concurrent generation of glycopeptide-specific α/β CTL and carbohydrate-specific γ/δ CTL.

Implications for T Cell Recognition of Natural Glycopeptides

Glycosylation of secreted, cell surface, nuclear, and cytoplasmic proteins (Hart et al., 1989) is a common posttranslational modification that plays a crucial role in molecular structure and stability, masking of microorganism target epitopes, and modulation of specific protein functions (Varki, 1993). The small number of natural MHC I bound glycopeptides that have been identified may reflect their limited numbers at the cell surface or the technical difficulties in their detection (Haurum et al., 1994), but not necessarily their importance in the cellular immune response since T cell avidity for pMHC antigens widely varies. Our results, together with those from other studies of glycopeptide immunogenicity, suggest small carbohydrates (mono or disaccharides) attached to short, centrally placed linkers satisfy α/β TCR antigen binding preferences, and that carbohydrates of the same size attached to slightly longer linkers may also satisfy the requirements for γ/δ TCR antigen binding (Figure 4), leading to glycopeptide and carbohydrate-specific T cell responses. Asparagine-linked glycans have a pentasaccharide core decorated by further carbohydrate additions (Kornfeld and Kornfeld, 1985); therefore, the corresponding glycopeptides would not be well suited for carbohydrate-specific CTL. In contrast, many mucins and other O-linked glycoconjugates found in the cytoplasm and nucleus are composed of mono- or disaccharides attached to serine, threonine, hydroxylysine or tyrosine (Hart et al., 1989; Kihlberg and Elofsson, 1997) and, therefore, are more promising natural glycan antigens for T cells. The mucins, that include the Tn and sialyl Tn epitopes that are present on cancer cells and HIV envelope glycoprotein gp120 (Hansen et al., 1990), can be recognized by T cells (Galli-Stampino et al., 1997). Carbohydrate structures that are not well represented or are poorly immunogenic in normal antigen presentation could also be used in synthetic peptide immunogens to activate defined, carbohydrate-specific T cell populations. The ability to generate or enhance the Ig-like, MHC-unrestricted γ/δ T cell responses to the glycopeptide could further augment T cell surveillance and CTL effector functions against cells presenting the corresponding carbohydrate hapten. Indeed, peptide-based vaccines able to generate carbohydrate-specific CTL have potential clinical applications for treatment of various types of cancer and parasitic infections (Lanzavecchia, 1993; Chesnut et al., 1995) by targeting abnormal glycosylation produced by malignant cells or oligosaccharide structures unique to microorganisms (Kaufmann, 1996).

Experimental Procedures

Carbohydrates, Glycopeptides, and Glycolipids

Galabiose (Gal-α(1,4)Gal-β or Gal_2), CD77 (Gal-α(1,4)Gal-β(1,4)Glc-β), lactose (Gal-β(1,4)-Glc-β), GM3 (NeuAc-α(3)-GalN-β(1,4)Glc-β), and GM3-lactam were synthesized as described (Figure 1; Abdel-Motal et al., 1995; Kihlberg and Elofsson, 1997). Monoclonal antibodies specific for the carbohydrates were used to test the expression of carbohydrates on the surface of glycopeptide-treated RMA-S cells (Abdel-Motal et al., 1996).

Glycopeptides and glycolipids were synthesized and tested for K^b and D^b-binding capacity, carbohydrate presentation, and stability in vivo as described (Abdel-Motal et al., 1995, 1996).

CTL Generation, Assay, and Fractionation

CTL were generated by immunization of C57BL/6 mice with 100 μg glycopeptide in Freund's incomplete adjuvant at the base of the tail followed by in vitro restimulation of harvested spleen cells, as described (Zhou et al., 1992). CTL were tested in a short-term 4 hr ^{51}Cr-release assay against peptide-, glycopeptide- or glycolipid-treated target cells. Glycolipid-expressing target cells were produced by treatment of target cells with liposomes containing the different glycolipids as described (Abdel-Motal et al., 1995). CTL populations were fractionated using either anti-α/β or γ/δ framework MAb on magnetic Dynabeads (Dynal A. S., Norway).

Preparation and Crystallization of the K^b-Glycopeptide Complex

Purified H-2K^b was incubated with a 5-fold molar excess of RGY8-6H-Gal_2 for 5 hr at room temperature (see Stura et al., 1992). Centricon 10 ultrafiltration was used to concentrate the MHC complex and clear any free peptide simultaneously. An exchange of bound peptides was apparent from notable band shifts between treated and untreated samples subjected to IEF electrophoresis (data not shown; see also Stura et al., 1992). Large single crystals were grown from 18 mg/ml H-2K^b in 2.3 M Na/K PO_4, 2% 2-methyl-2,4-pentanediol (pH 6.4), with diffraction to approximately 2.0 Å resolution.

Data Collection and Processing

Diffraction data were collected in house from a flash-cooled (130 K, 25% glycerol) single crystal ($0.5 \times 0.5 \times 0.3$ mm) with a 30 cm MAR image plate mounted on a Siemens M18X CuKα x-ray generator (300 μm focal cup, 50 kV, 80 mA) fitted with Supper long double-mirror focusing optics. The data were indexed and integrated with the program DENZO (Otwinowski and Minor, 1997). The crystals are orthorhombic, $P2_12_12$, with unit cell dimensions a = 135.9 Å, b = 86.8 Å, and c = 45.0 Å. The V_m (Matthews, 1968) of 2.86 $Å^3$ Da^{-1} indicated one molecule per asymmetric unit with a solvent content of 57%. The data were merged, scaled, and reduced to a unique reflection set using the program SCALEPACK (Table 3; Otwinowski and Minor, 1997).

Model Refinement

A random set of 10% of the reflections between 18–2.1 Å were excluded from refinement to monitor R_{free} (Brünger, 1997). Only procedures that minimized both R_{cryst} and R_{free} were utilized. K^b/VSV-8 coordinates (Fremont et al., 1992) stripped of peptide were directly refined against the glycopeptide data using X-PLOR v3.851 (Brünger et al., 1987). Rigid body refinement from 8–2.1 Å resolution ($F/\sigma_F > 2$) gave an R_{cryst} of 36.6% and an R_{free} of 35.7%. One round of refinement, bulk-solvent correction, and model rebuilding was performed using positional minimization and iterative slow-cooled molecular dynamics as implemented in X-PLOR (serial slow cool, Kleywegt and Jones, 1997) before the peptide was traced (R_{cryst} 27.5%, R_{free} 32.5%). $3F_o$-$2F_c$, $2F_o$-F_c shake omit (McRee, 1993), and shaken, σ_A-weighted (Read, 1986) $2F_o$-F_c and F_o-F_c electron density maps were computed to reduce phase bias for model rebuilding. Strong density in shaken, σ_A-weighted F_o-F_c maps was located within the peptide binding groove and included the entire glycosylated homocysteine at position six (HggP6; Figure 2). HggP6 was constructed with the help of the hetero-compound libraries (e.g., homocysteine and galactose) provided by G. Kleywegt's web site (http://alpha2.bmc.uu.se/hicup; Kleywegt, 1995). The R_{free} for the outer reflection bin failed to decline, probably due to limited data completeness; therefore, the high resolution limit was reduced to 2.2 Å (Table 3). The coordinates and reflection data (keeping the same R_{free} data partition) were converted for use in the SHELXL automated water divining routine (Sheldrick and Schneider, 1997) and 108 waters were retained after manual inspection. The final rounds of positional and B-value refinement in X-PLOR gave an R_{cryst} of 22.4% and an R_{free} of 27.9% (Table 3).

Table 3. X-Ray Data Processing and Refinement Statistics for the H-2K^b Glycopeptide Complex

Data Processing		
	(All Data)	(Outer Shell)
Resolution range (Å)	20–2.1	2.17–2.1
Unique Reflections	28511	1734
Completeness (%)	89.3	55.0
R_{merge} (%)[a]	7.8	38.4
Average I/σ_1	16.2	1.9
Redundancy[b]	5.4	1.7
Refinement[c]		
Resolution range (Å)	18–2.2	2.3–2.2
R_{cryst}[d] (no. of refls)	0.224 (23515)	0.368 (2374)
R_{free}[d] (no. of refls)	0.279 (2605)	0.422 (266)
Number of atoms[e] (C^α atoms)	3304 (381)	
Water molecules: 108	N-linked carbohydrates: 4	
Coordinate error[f]: 0.38Å	Real space CC[g]: 0.90	

Protein Geometry and Thermal Parameters			
R.m.s. deviation from ideality:		Ramachandram Plot:	
bonds	0.008Å	favored	89.2%
angles	1.4°	allowed	10.2%
dihedrals	26.2°	generous	0.6%
impropers	1.3°	disallowed	0%
Average B-values ($Å^2$):			
all atoms	31	carbohydrates	58
peptide	35	waters	37

The space group is $P2_12_12$ with one molecule per asymmetric unit. The unit cell dimensions are a = 135.9 Å, b = 86.8 Å, c = 45.0 Å.

[a] $R_{merge} = (\Sigma_h\Sigma_i (I_{hi} - <I_h>)/\Sigma_h\Sigma_i I_h) \times 100$ where $<I_h>$ is the mean of the I_{hi} observations of reflection h.

[b] Redundancy = < # of observations / # of unique reflections >.

[c] Statistics for all data with $F/\sigma_F \geq 0$.

[d] $R_{cryst} = (\Sigma_h|F_o - F_c| / \Sigma_h F_o)$ where F_o and F_c are the observed and calculated structure factors; R_{free} is R_{cryst} computed with only the test set structure factors.

[e] Number for all non-hydrogen atoms, including the waters and carbohydrates.

[f] Estimated from cross-validated Luzzati plots (Luzzati, 1952) using a low resolution limit of 5 Å.

[g] Correlation coefficient (CC) computed for all protein atoms with program O (Jones et al., 1991).

Structural Analysis and Illustrations

The H-2K^b glycopeptide structure was compared with other K^b/peptide complexes (PDB accession codes 2VAA, 2VAB; Fremont et al., 1992), the H-2D^b/peptide complex (1HOC, Young et al., 1994), the H-2L^d/peptide complex (1LDP, Speir et al., 1998), the HLA-A2/Influenza M1 peptide complex (1HHI, Madden et al., 1993), and various complexes of HIV-derived peptides bound to HLA molecules B35, B53, and B8 (1AGE, Reid et al., 1996; 1A1M, Smith et al., 1996a; 1A1N, Smith et al., 1996b). PROCHECK (Laskowski et al., 1993) was used to examine polypeptide geometry, PROMOTIF to identify secondary structure elements (Hutchinson and Thornton, 1996), CONTACSYM (Sheriff et al., 1987) to identify van der Waals contacts up to 4 Å apart, and HBPLUS (McDonald and Thornton, 1994) to locate hydrogen bond pairs using both distance and geometry criteria. Buried surface areas were computed with MS (Connolly, 1983) using a 1.4 Å radius probe. Figure 2 was created using programs O (Jones et al., 1991) and MolView (Smith, 1995). Figure 3 was created using MIDAS (Ferrin et al., 1988).

Acknowledgments

We thank Wendy Havran for critically reading the manuscript and helpful discussions, Andreas Heine for assistance with program SHELXL, and David Jewell for technical assistance. This study was supported by National Institutes of Health grants CA58896 (I. A. W.), AI42266 (I. A. W.), and a postdoctoral fellowship from National Institutes of Health training grant MH19185 (J. A. S.). This is manuscript #11737-MB from The Scripps Research Institute.

Received October 23, 1998; revised December 2, 1998.

References

Abdel-Motal, U.M., Zhou, X., Joki, A., Siddiqi, A.R., Srinivasa, B.R., Stenvall, K., Dahmén, J., and Jondal, M. (1993). Major histocompatibility complex class I-binding peptides are recycled to the cell surface after internalization. Eur. J. Immunol. *23*, 3224–3229.

Abdel-Motal, U.M., Berg, L., Bengtsson, M., Dahmén, J., Kihlberg, J., Magnusson, G., Nilsson, U., and Jondal, M. (1995). Major histocompatibility complex class I binding glycopeptides for the estimation of "empty" class I molecules. J. Immunol. Methods *188*, 21–31.

Abdel-Motal, U.M., Berg, L., Rosen, A., Bengtsson, M., Thorpe, C.J., Kihlberg, J., Dahmén, J., Magnusson, G., Karlsson, K.A., and Jondal, M. (1996). Immunization with glycosylated K^b-binding peptides generates carbohydrate-specific, unrestricted cytotoxic T cells. Eur. J. Immunol. *26*, 544–551.

Beckman, E.M., Porcelli, S.A., Morita, C.T., Behar, S.M., Furlong, S.T., and Brenner, M.B. (1994). Recognition of a lipid antigen by CD1-restricted $\alpha\beta+$ T cells. Nature *372*, 691–694.

Boismenu, R., and Havran, W.L. (1997). An innate view of $\gamma\delta$ T cells. Curr. Opin. Immunol. *9*, 57–63.

Broddefalk, J., Backlund, J., Almqvist, F., Johansson, M., Holmdahl, R., and Kihlberg, J. (1998). T cells recognize a glycopeptide derived from type II collagen in a model for rheumatoid arthritis. J. Am. Chem. Soc. *120*, 7676–7683.

Brünger, A.T. (1997). The free R value: a more objective statistic for crystallography. Methods Enzymol. *277*, 366–396.

Brünger, A.T., Kuriyan, J., and Karplus, M. (1987). Crystallographic *R* factor refinement by molecular dynamics. Science *235*, 458–460.

Carbone, F.R., and Gleeson, P.A. (1997). Carbohydrates and antigen recognition by T cells. Glycobiology *7*, 725–730.

Chesnut, R.W., Sette, A., Celis, E., Wentworth, P., Kubo, R.T., Alexander, J., Ishioka, G., Vitiello, A., and Grey, H.M. (1995). Design and testing of peptide-based cytotoxic T cell-mediated immunotherapeutics to treat infectious diseases and cancer. Pharm. Biotechnol. *6*, 847–874.

Chien, Y.H., Jores, R., and Crowley, M.P. (1996). Recognition by γ/δ T cells. Annu. Rev. Immunol. *14*, 511–532.

Connolly, M.L. (1983). Solvent-accessible surfaces of proteins and nucleic acids. Science *221*, 709–713.

Davis, M.M., and Chien, Y. (1995). Issues concerning the nature of antigen recognition by $\alpha\beta$ and $\gamma\delta$ T cell receptors. Immunol. Today *16*, 316–318.

Davis, M., Boniface, J., Reich, Z., Lyons, D., Hampl, J., Arden, B., and Chien, Y. (1998). Ligand recognition by $\alpha\beta$ T cell receptors. Annu. Rev. Immunol. *16*, 523–544.

Ding, Y.H., Smith, K.J., Garboczi, D.N., Utz, U., Biddison, W.E., and Wiley, D.C. (1998). Two human T cell receptors bind in a similar diagonal mode to the HLA-A2/Tax peptide complex using different TCR amino acids. Immunity *8*, 403–411.

Eisen, H.N., Sykulev, Y., and Tsomides, T.J. (1996). Antigen-specific T-cell receptors and their reactions with complexes formed by peptides with major histocompatibility complex proteins. Adv. Protein Chem. *49*, 1–56.

Ferrin, T.E., Huang, C.C., Jarvis, L.E., and Langridge, R. (1988). The MIDAS display system. J. Mol. Graph. *6*, 13–27.

Fremont, D.H., Matsumura, M., Stura, E.A., Peterson, P.A., and Wilson, I.A. (1992). Crystal structures of two viral peptides in complex with murine MHC class I H-$2K^b$. Science *257*, 919–927.

Galli-Stampino, L., Meinjohanns, E., Frische, K., Meldal, M., Jensen, T., Werdelin, O., and Mouritsen, S. (1997). T-cell recognition of tumor-associated carbohydrates: the nature of the glycan moiety plays a decisive role in determining glycopeptide immunogenicity. Cancer Res. *57*, 3214–3222.

Garboczi, D.N., Ghosh, P., Utz, U., Fan, Q.R., Biddison, W.E., and Wiley, D.C. (1996). Structure of the complex between human T-cell receptor, viral peptide and HLA-A2. Nature *384*, 134–141.

Garcia, K.C., Degano, M., Stanfield, R.L., Brunmark, A., Jackson, M.R., Peterson, P.A., Teyton, L., and Wilson, I.A. (1996). An $\alpha\beta$ T cell receptor structure at 2.5Å and its orientation in the TCR-MHC complex. Science *274*, 209–219.

Garcia, K.C., Degano, M., Pease, L.R., Huang, M., Peterson, P.A., Teyton, L., and Wilson, I.A. (1998). Structural basis of plasticity in T-cell receptor recognition of a self peptide-MHC antigen. Science *279*, 1166–1172.

Hakomori, S. (1989). General concept of tumor-associated carbohydrate antigens: their chemical, physical, and enzymatic basis. In Gangliosides and Cancer, H.F. Oettgen, ed. (Weinheim, Germany: VCH), pp. 57–68.

Hansen, J.E., Clausen, H., Nielsen, C., Teglbjaerg, L.S., Hansen, L.L., Nielsen, C.M., Dabelsteen, E., Mathiesen, L., Hakomori, S.I., and Nielsen, J.O. (1990). Inhibition of human immunodeficiency virus (HIV) infection in vitro by anticarbohydrate monoclonal antibodies: peripheral glycosylation of HIV envelope glycoprotein gp120 may be a target for virus neutralization. J. Virol. *64*, 2833–2840.

Hart, G.W., Haltiwanger, R.S., Holt, G.D., and Kelly, W.G. (1989). Glycosylation in the nucleus and cytoplasm. Annu. Rev. Biochem. *58*, 841–874.

Haurum, J.S., Arsequell, G., Lellouch, A.C., Wong, S.Y., Dwek, R.A., McMichael, A.J., and Elliott, T. (1994). Recognition of carbohydrate by major histocompatibility complex class I-restricted, glycopeptide-specific cytotoxic T lymphocytes. J. Exp. Med. *180*, 739–744.

Hochgeschwender, U., Simon, H.G., Weltzien, H.U., Bartels, F., Becker, A., and Epplen, J.T. (1987). Dominance of one T-cell receptor in the H-$2K^b$/TNP response. Nature *326*, 307–309.

Holmes, E.H., Hakomori, S., and Ostrander, G.K. (1987). Synthesis of type 1 and 2 lacto series glycolipid antigens in human colonic adenocarcinoma and derived cell lines is due to activation of a normally unexpressed β(1–3) N-acetylglucosaminyltransferase. J. Biol. Chem. *262*, 15649–15658.

Hutchinson, E.G., and Thornton, J.M. (1996). PROMOTIF-a program to identify and analyze structural motifs in proteins. Prot. Sci. *5*, 212–220.

Ishioka, G.Y., Lamont, A.G., Thomson, D., Bulbow, N., Gaeta, F.C., Sette, A., and Grey, H.M. (1992). MHC interaction and T cell recognition of carbohydrates and glycopeptides. J. Immunol. *148*, 2446–2451.

Jones, T.A., Cowan, S., Zou, J.Y., and Kjeldgaard, M. (1991). Improved methods for building protein models in electron density maps and the location of errors in these models. Acta Cryst. *A47*, 110–119.

Kaufmann, S.H. (1996). $\gamma\delta$ and other unconventional T lymphocytes: what do they see and what do they do? Proc. Natl. Acad. Sci. USA *93*, 2272–2279.

Kihlberg, J., and Elofsson, M. (1997). Solid-phase synthesis of glycopeptides: immunological studies with T cell stimulating glycopeptides. Curr. Med. Chem. *4*, 85–116.

Kleywegt, G.J. (1995). Dictionaries for Heteros. ESF/CCP4 Newsletter *31*, 45–50.

Kleywegt, G.J., and Jones, T.A. (1997). Model building and refinement practice. Methods Enzymol. *277*, 208–230.

Kohler, J., Hartmann, U., Grimm, R., Pflugfelder, U., and Weltzien, H.U. (1997). Carrier-independent hapten recognition and promiscuous MHC restriction by CD4 T cells induced by trinitrophenylated peptides. J. Immunol. *158*, 591–597.

Kornfeld, R., and Kornfeld, S. (1985). Assembly of asparagine-linked oligosaccharides. Annu. Rev. Biochem. *54*, 631–664.

Lanzavecchia, A. (1993). Identifying strategies for immune intervention. Science *260*, 937–944.

Laskowski, R.A., MacArthur, M.W., Moss, D.S., and Thornton, J.M. (1993). PROCHECK: a program to check the stereochemical quality of protein structures. J. Appl. Cryst. *26*, 283–291.

Luzzati, V. (1952). Traitement statistique des erreurs dans la determination des structures cristallines. Acta Cryst. *5*, 802–810.

Madden, D.R., Garboczi, D.N., and Wiley, D.C. (1993). The antigenic identity of peptide-MHC complexes: a comparison of the conformations of five viral peptides presented by HLA-A2. Cell *75*, 693–708.

Martin, S., Ortmann, B., Pflugfelder, U., Birsner, U., and Weltzien, H.U. (1992). Role of hapten-anchoring peptides in defining hapten-epitopes for MHC-restricted cytotoxic T cells. Cross-reactive TNP-determinants on different peptides. J. Immunol. *149*, 2569–2575.

Matthews, B.W. (1968). Solvent content of protein crystals. J. Mol. Biol. *33*, 491–497.

McDonald, I.K., and Thornton, J.M. (1994). Satisfying hydrogen bonding potential in proteins. J. Mol. Biol. *238*, 777–793.

McRee, D.E. (1993). Practical protein crystallography (San Diego: Academic Press, Inc), pp. 225, 273.

Melian, A., Beckman, E.M., Porcelli, S.A., and Brenner, M.B. (1996). Antigen presentation by CD1 and MHC-encoded class I-like molecules. Curr. Opin. Immunol. *8*, 82–88.

Nores, G.A., Dohi, T., Taniguchi, M., and Hakomori, S. (1987). Density-dependent recognition of cell surface GM3 by a certain anti-melanoma antibody, and GM3 lactone as a possible immunogen: requirements for tumor-associated antigen and immunogen. J. Immunol. *139*, 3171–3176.

Nudelman, E., Kannagi, R., Hakomori, S., Parsons, M., Lipinski, M., Wiels, J., Fellous, M., and Tursz, T. (1983). A glycolipid antigen associated with Burkitt lymphoma defined by a monoclonal antibody. Science *220*, 509–511.

Otwinowski, Z., and Minor, W. (1997). Processing of x-ray diffraction data collected in oscillation mode. Methods Enzymol. *276*, 307–326.

Porcelli, S.A., Morita, C.T., and Modlin, R.L. (1996). T-cell recognition of non-peptide antigens. Curr. Opin. Immunol. *8*, 510–516.

Porcelli, S.A., Segelke, B.W., Sugita, M., Wilson, I.A., and Brenner, M.B. (1998). The CD1 family of lipid antigen-presenting molecules. Immunol. Today *19*, 362–368.

Rammensee, H.G., Falk, K., and Rotzschke, O. (1993). Peptides naturally presented by MHC class I molecules. Annu. Rev. Immunol. *11*, 213–244.

Rammensee, H.G., Friede, T., and Stevanoviic, S. (1995). MHC ligands and peptide motifs: first listing. Immunogenetics *41*, 178–228.

Read, R.J. (1986). Improved fourier coefficients for maps using phases from partial structures with errors. Acta Cryst. *A42*, 140–149.

Reid, S.W., McAdam, S., Smith, K.J., Klenerman, P., O'Callaghan, C.A., Harlos, K., Jakobsen, B.K., McMichael, A.J., Bell, J.I., Stuart, D.I., and Jones, E.Y. (1996). Antagonist HIV-1 Gag peptides induce structural changes in HLA-B8. J. Exp. Med. *184*, 2279–2286.

Rock, E.P., Sibbald, P.R., Davis, M.M., and Chien, Y.H. (1994). CDR3 length in antigen-specific immune receptors. J. Exp. Med. *179*, 323–328.

Schumacher, T.N., De Bruijn, M.L., Vernie, L.N., Kast, W.M., Melief, C.J., Neefjes, J.J., and Ploegh, H.L. (1991). Peptide selection by MHC class I molecules. Nature *350*, 703–706.

Sheldrick, G.M., and Schneider, T.R. (1997). SHELXL: high-resolution refinement. Methods Enzymol. *277*, 319–343.

Sheriff, S., Hendrickson, W.A., and Smith, J.L. (1987). Structure of myohemerythrin in the azidomet state at 1.7/1.3Å resolution. J. Mol. Biol. *197*, 273–296.

Sieling, P.A., Chatterjee, D., Porcelli, S.A., Prigozy, T.I., Mazzaccaro, R.J., Soriano, T., Bloom, B.R., Brenner, M.B., Kronenberg, M., Brennan, P.J., et al. (1995). CD1-restricted T cell recognition of microbial lipoglycan antigens. Science *269*, 227–230.

Smith, K.J., Reid, S.W., Harlos, K., McMichael, A.J., Stuart, D.I., Bell, J.I., and Jones, E.Y. (1996a). Bound water structure and polymorphic amino acids act together to allow the binding of different peptides to MHC class I HLA-B53. Immunity *4*, 215–228.

Smith, K.J., Reid, S.W., Stuart, D.I., McMichael, A.J., Jones, E.Y., and Bell, J.I. (1996b). An altered position of the α_2 helix of MHC class I is revealed by the crystal structure of HLA-B*3501. Immunity *4*, 203–213.

Smith, T.J. (1995). MolView: a program for analyzing and displaying atomic structures on the Macintosh personal computer. J. Mol. Graph. *13*, 122–125.

Speir, J.A., Garcia, K.C., Brunmark, A., Degano, M., Peterson, P.A., Teyton, L., and Wilson, I.A. (1998). Structural basis of 2C TCR allorecognition of H-2L^d peptide complexes. Immunity *8*, 553–562.

Stura, E.A., Matsumura, M., Fremont, D.H., Saito, Y., Peterson, P.A., and Wilson, I.A. (1992). Crystallization of murine major histocompatibility complex class I H-2K^b with single peptides. J. Mol. Biol. *228*, 975–982.

Svensson, G., Albertsson, J., Svensson, C., Magnusson, G., and Dahmen, J. (1986). X-ray crystal structure of galabiose, O-α-D-galactopyranosyl-(1-4)-D-galactopyranose. Carbohydr. Res. *146*, 29–38.

van Bleek, G.M., and Nathenson, S.G. (1990). Isolation of an endogenously processed immunodominant viral peptide from the class I H-2K^b molecule. Nature *348*, 213–216.

Varki, A. (1993). Biological roles of oligosaccharides: all of the theories are correct. Glycobiology *3*, 97–130.

Wilson, I.A., and Stanfield, R.L. (1994). Antibody-antigen interactions: new structures and new conformational changes. Curr. Opin. Struct. Biol. *4*, 857–867.

Wilson, I.A., and Garcia, K.C. (1997). T cell receptor structure and TCR complexes. Curr. Opin. Struct. Biol. *7*, 839–848.

Young, A.C., Zhang, W., Sacchettini, J.C., and Nathenson, S.G. (1994). The three-dimensional structure of H-2D^b at 2.4Å resolution: implications for antigen-determinant selection. Cell *76*, 39–50.

Zeng, Z., Castaño, A.R., Segelke, B.W., Stura, E.A., Peterson, P.A., and Wilson, I.A. (1997). Crystal structure of mouse CD1: an MHC-like fold with a large hydrophobic binding groove. Science *277*, 339–345.

Zhou, X., Berg, L., Motal, U.M., and Jondal, M. (1992). In vivo primary induction of virus-specific CTL by immunization with 9mer synthetic peptides. J. Immunol. Methods *153*, 193–200.

Brookhaven Protein Data Bank ID Codes

Coordinates for the K^b-RGY8-6H-Gal$_2$ complex have been deposited in the Protein Data Bank (Brookhaven, NY) with accession code 1KBG.